nature communications

Article

https://doi.org/10.1038/s41467-026-74899-9

Human wastewater contamination drives the emergence of multidrug-resistant bacteria in the Galápagos marine ecosystem

Received: 22 September 2025

Accepted: 1 June 2026

Published online: 04 August 2026

Check for updates

Arnav Lal[1,2,3], Jade C. Riopelle[1,3], Katherine Villarin[1,3], Maya Mathur[1,3], Lia Enriquez[3,4], Rui Xiao[1], Naomi Phemister-Jimenez[1,3], Katherine Gilbert[1,3], Stephen D. Cole[1], Maddie Tilyou[4], Kelly P. Kennedy[4], Ernesto Vaca[5], Wilson Castillo[5], Michael Weisberg[4,6], Lisa M. Mattei[1,7] ✉ & Daniel P. Beiting[1,7] ✉

Antimicrobial resistance poses a global threat to public health. Mobile microbiological laboratories can enable environmental monitoring of antimicrobial resistance, particularly in geographically remote and resource-limited locations, such as the Galápagos archipelago. Here, we report the development of a mobile laboratory for antimicrobial resistance surveillance of marine sites surrounding San Cristóbal, the archipelago's second most populated island, which has experienced rapid urbanization and intense international tourism pressure. On-site metagenomic sequencing of wastewater-contaminated marine sites reveals a stark shift in microbial genera and a higher count of antimicrobial resistance genes compared to uncontaminated marine sites, mirroring metagenomic results of local untreated sewage. Over 40% of lactose-fermenting *Enterobacteriaceae* isolates collected directly from sewage or marine environments near sites of wastewater outfall exhibit multidrug resistance. Long-read sequencing and de novo assembly of bacterial genomes and plasmids from multidrug-resistant *Escherichia coli* reveal frequent and rapid reassortment of antimicrobial resistance genes on plasmids, generating a diverse and functional resistome on the island. This study not only provides a framework for conducting antimicrobial resistance research in low-resource settings but also underscores the impact of wastewater contamination on the environmental antimicrobial resistance landscape and highlights potential threats to human and animal health.

Antimicrobial resistance (AMR) is a major threat to global public health. In 2021, bacterial AMR was associated with roughly 5 million deaths worldwide—accounting for 9% of all deaths—and this burden is projected to double by 2050[1]. Lower- and middle-income countries (LMICs) are disproportionately affected by AMR due to myriad factors, including inadequate surveillance and waste management infrastructure, lower vaccination rates, rapidly developing agricultural practices, increased urbanization, and antimicrobial misuse[2–5]. Despite the global importance of AMR, the mechanisms and pathways of AMR dissemination in the environment remain poorly understood. This knowledge gap is particularly severe in LMICs, where limited access to modern laboratory infrastructure, reliable power, and cold chain storage hinders surveillance efforts.

A full list of affiliations appears at the end of the paper. ✉e-mail: lmattei@upenn.edu; beiting@upenn.edu

Mobile sequencing technology offers an opportunity to begin addressing this gap. For example, the Zika in Brazil Real Time Analysis (ZIBRA) project demonstrated that Oxford Nanopore sequencing could be used for Zika virus genomic epidemiology in near-real time, clarifying geographic spread and transmission patterns during the 2015 outbreak in South America[6]. Similarly, nanopore-based sequencing is now enabling rapid, field-deployable AMR surveillance of environmental samples, including real-time detection of AMR genes[7] and whole-genome sequencing of phenotypically resistant species[8,9]. However, targeted sequencing is only one of many assessment tools for developing a complete understanding of the geographic and genomic dynamics of environmental AMR. Other techniques, including qPCR-based surveillance, culture-dependent AMR phenotyping of isolates, and untargeted metagenomic sequencing, can provide complementary insights into the drivers and mechanisms of resistance and AMR transmission. Unfortunately, current strategies to develop "mini-labs" for AMR surveillance in LMICs focus primarily on culture-based analyses, and require significant space and time for set-up[10], thus underscoring the need for a multimodal approach that can be set-up on any countertop or folding table.

The Galápagos archipelago is an ideal natural laboratory for studying how human activity affects the emergence and evolution of AMR in marine ecosystems. Although the majority of the archipelago's islands remain uninhabited, four have small but growing human populations, with most residents settled on the islands of Santa Cruz and San Cristóbal (~17,000 and 8300, respectively, as of the 2022 census[11]). Both islands have experienced rapid urbanization, with annual population growth rates of 6%—three times the rate of mainland Ecuador—and both face intense pressure from land-based national and international tourism. In 2022, for example, San Cristóbal recorded more than 76,000 tourist visits to areas within a 2.5 km radius of Puerto Baquerizo Moreno, the island's largest town[11,12]. Altogether, these societal trends highlight the 'Galápagos Paradox'—the observation that while tourism provides essential support for the local economy and funds conservation efforts, it simultaneously spurs population growth and poses a threat to the delicate biodiversity and ecosystems that form the entire basis of the tourism industry in the archipelago[13]. This is particularly concerning in the context of AMR, because international tourism and resident population growth are likely increasing the abundance and diversity of antimicrobials and AMR-containing bacteria within the archipelago.

Human wastewater contamination of coastal waters is a global problem[14], and previous studies have linked AMR in the environment to wastewater treatment plant (WWTP) inputs[15–17]. Inadequate wastewater management on San Cristóbal has been highlighted as a source of fecal coliform contamination and AMR in recreational waters[18–20]. San Cristóbal is the only Galápagos island with a functional WWTP[18], which was originally constructed in 1982 and became fully operational around 2012—likely delayed by logistical challenges, including the transition from septic tanks and the difficulty of burying pipes in volcanic rock. The system was designed as a combined sewer overflow that relies on three pumping stations to move raw sewage from the population center located at sea level to a WWTP at a higher elevation (Supplementary Fig. 1). Unfortunately, the WWTP has not been updated since its construction, even as the island's human population has quadrupled, leaving the system routinely overwhelmed and prone to mechanical failure[21]. For example, between August 2019 and December 2020, failure of the WWTP on San Cristobal resulted in the discharge of over 600,000 cubic meters of untreated sewage into the surrounding coastal waters[19]. A 2020 study of the WWTP reported that removal efficiencies for ammonium, phosphate, sulfur, total solids, total suspended solids, and turbidity were all within Ecuadorian standards for discharge into marine waters, suggesting a functioning WWTP[18]. However, the same study reported that the WWTP had no effect on total coliforms or *E. coli* counts, resulting in effluent that was 25 times the Ecuadorian standard of 2000 Most Probable Number (MPN)/100 mL for *E. coli*. Despite meeting some regulatory standards for certain pollutants, the outdated and overburdened wastewater treatment system on San Cristóbal continues to pose significant environmental and public health risks due to its failure to effectively remove fecal indicator bacteria like *E. coli* from effluent.

Despite these unique circumstances, little is known about the impact of untreated wastewater contamination on the Galápagos' marine environment. Although several studies have examined water quality on and around the islands, only a single study evaluated AMR in fecal coliforms, but it was limited to a small number of narrow-spectrum antimicrobials without genotyping of AMR isolates, thus providing an incomplete picture of the environmental "resistome" in the Galápagos. To address this knowledge gap, we developed a mobile microbiology laboratory to identify sites of untreated wastewater contamination and link bacterial taxa, AMR genes, and resistance phenotypes. We used a multimodal approach performed on-site without access to a centralized laboratory. A fecal qPCR assay identified hot spots of untreated wastewater contamination, while untargeted shotgun metagenomic sequencing of marine water identified human fecal taxa and AMR gene profiles that matched what was observed contemporaneously in local untreated municipal sewage. Moreover, lactose-fermenting *Enterobacteriaceae* selectively cultured from contaminated marine environments frequently exhibited multidrug resistance (MDR) phenotypes, and whole-genome sequencing of *E. coli* strains revealed rapid and frequent reassortment of AMR genes within plasmids, ultimately giving rise to potentially novel MDR bacteria. Taken together, these data underscore the need for environmental AMR surveillance and risk assessment in the Galápagos archipelago to protect residents, tourists, and the marine ecosystem. Our mobile laboratory provides a model for a comprehensive environmental AMR surveillance platform that can be deployed in resource-limited settings.

Results

Identifying sites of persistent wastewater contamination

Traditional microbiology and microbial genomic laboratories occupy a large footprint and are highly dependent on a reliable cold chain and continuous electrical supply. Most research instrumentation is not meant to operate outside of this environment, and consumables such as media plates and plasticware may not be readily available in LMICs. These factors restrict robust environmental surveillance of AMR to areas close to well-resourced laboratories. To circumvent these issues, we developed and optimized a mobile microbiology field laboratory (Supplementary Data 1) that allowed us to detect wastewater contamination in marine ecosystems (Fig. 1A), isolate bacterial strains for AMR profiling (Fig. 1B), and carry out untargeted metagenomic sequencing and whole-genome sequencing of bacterial isolates (Fig. 1C).

To identify enteric pathogens in the marine ecosystem surrounding San Cristóbal, samples were collected over a two-year period from 16 marine sites, two freshwater sites, and two sites in the municipal wastewater treatment system that contain raw sewage (Supplementary Data 2). Sampling sites were distributed around the island (Fig. 2A), with the highest density within 1.5 km of the center of Puerto Baquerizo Moreno (Fig. 2B). Notably, this region is the epicenter of residential development and tourism on the island and includes five sites where untreated wastewater is known to be discharged into the environment. Four (Muelle de Pescadores, Laguna, Playa de los Marinos, Playa de Oro) are near WWTP pumping stations and excess-flow drains, and the other (Punta Carola Pipe) is a wastewater effluent discharge pipe that can release either treated or untreated waste depending on the state of the system (Supplementary Fig. 1). Six sites (Tongo Reef, Playa Lobería, Playa Baquerizo, Playa Mann, Playa Punta Carola, Muelle Tijeretas) are recreational beaches frequented by locals

https://doi.org/10.1038/s41467-026-74899-9

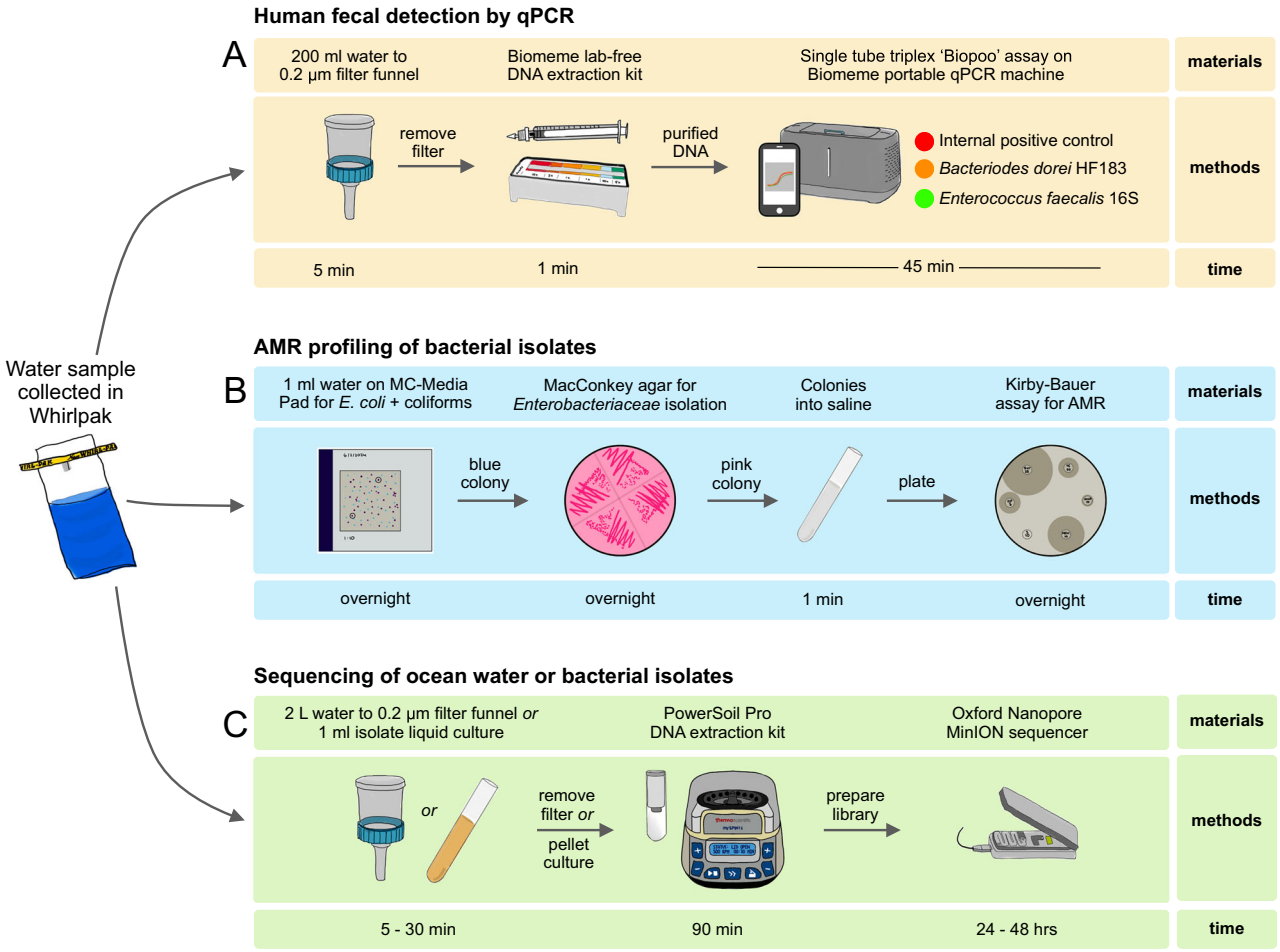

Fig. 1 | A mobile AMR discovery platform. Ocean water samples collected in sterile bags were processed through one or more of three workflows, each emphasizing field-ready assays and portable equipment: **A** qPCR for the detection of human fecal contamination. **B** AMR profiling of lactose-fermenting *Enterobacteriaceae* isolates from marine ecosystems or municipal sewer systems. **C** Long-read sequencing of ocean water, wastewater, or *E. coli* isolates. Consumables and equipment for workflows (**A**–**C**), along with associated costs, can be found in Supplementary Data 1. Figure was created using the vector graphics editor, Sketch.

and tourists and are located within 3 km of the town center. In contrast, four other sites (León Dormido, Puerto Chino, Bahía Rosa Blanca, and Punta Pitt) are distant tourist locations situated more than 15 km from the town center, and one site (Isla Española) is located off the coast of an unpopulated island ~50 km south of San Cristóbal (Fig. 2A).

Fecal contamination was evaluated using field-deployable, "lab-free" techniques. A hand pump was used to filter water, and DNA was extracted from material retained on the filter using a pipette- and centrifuge-free system (Biomeme), which employs pre-filled reagent cartridges and a syringe-based extraction column. Fecal contamination was screened for presence/absence using a field-ready lyophilized triplex qPCR assay that distinguishes a universal stool marker (*Enterococcus faecalis*) from a human-specific stool marker (the HF183 gene derived from *Bacteroides dorei* 16S rRNA) (Fig. 1A)[22]. Finally, qPCRs were run on the Franklin 'three9' (Biomeme), a portable, battery-powered thermocycler controlled via a smartphone app. Unsurprisingly, all samples tested positive for the universal stool marker by qPCR. Samples positive for the universal stool marker and negative for the human-specific stool marker suggest animal fecal contamination, consistent with the observation that all sites were frequented by marine species, most notably sea lions, marine iguanas, and a diverse array of fish and avian species. Multiple sites also tested positive for the human-specific stool marker, consistent with contamination from untreated sewage. We observed variability in human fecal qPCR signal over the sites and times our samples were collected (Fig. 2B, C), with the strongest and most consistent signal observed at the Punta Carola Pipe, a site in the vicinity of the intended outfall for treated sewage, but which has been locally confirmed and previously reported to be a point of outfall for untreated sewage (Supplementary Fig. 1)[20].

Other sampled sites exhibited lower and/or more variable qPCR detection of human stool. At Playa de Oro, a beach popular with sea lions and the site of a WWTP pumping station and excess-flow drain, high and low human qPCR findings are observed throughout both summers. The same pattern was also observed at Laguna, a brackish-water site near a different WWTP pumping station and excess-flow drain. At Muelle de Pescadores, a fishing pier and boat dock where residents occasionally swim, high levels of human fecal contamination were detected by qPCR during the first half of summer 2023 and throughout summer 2024, but not during the second half of summer 2023. While human fecal contamination was occasionally detected at other sites, it rarely reached the frequency of detection observed at Punta Carola Pipe, Playa de Oro, Muelle de Pescadores, or the Laguna. Notably, close proximity to a site with a strong human stool qPCR signal did not guarantee that a site would also be positive by qPCR. For example, the strong and consistently positive qPCR tests at Punta Carola Pipe were not reflected at nearby Playa Punta Carola, where qPCR signal was low and sporadic, perhaps due to the presence of an extended rocky breakwater separating the area where sewage outfall

https://doi.org/10.1038/s41467-026-74899-9

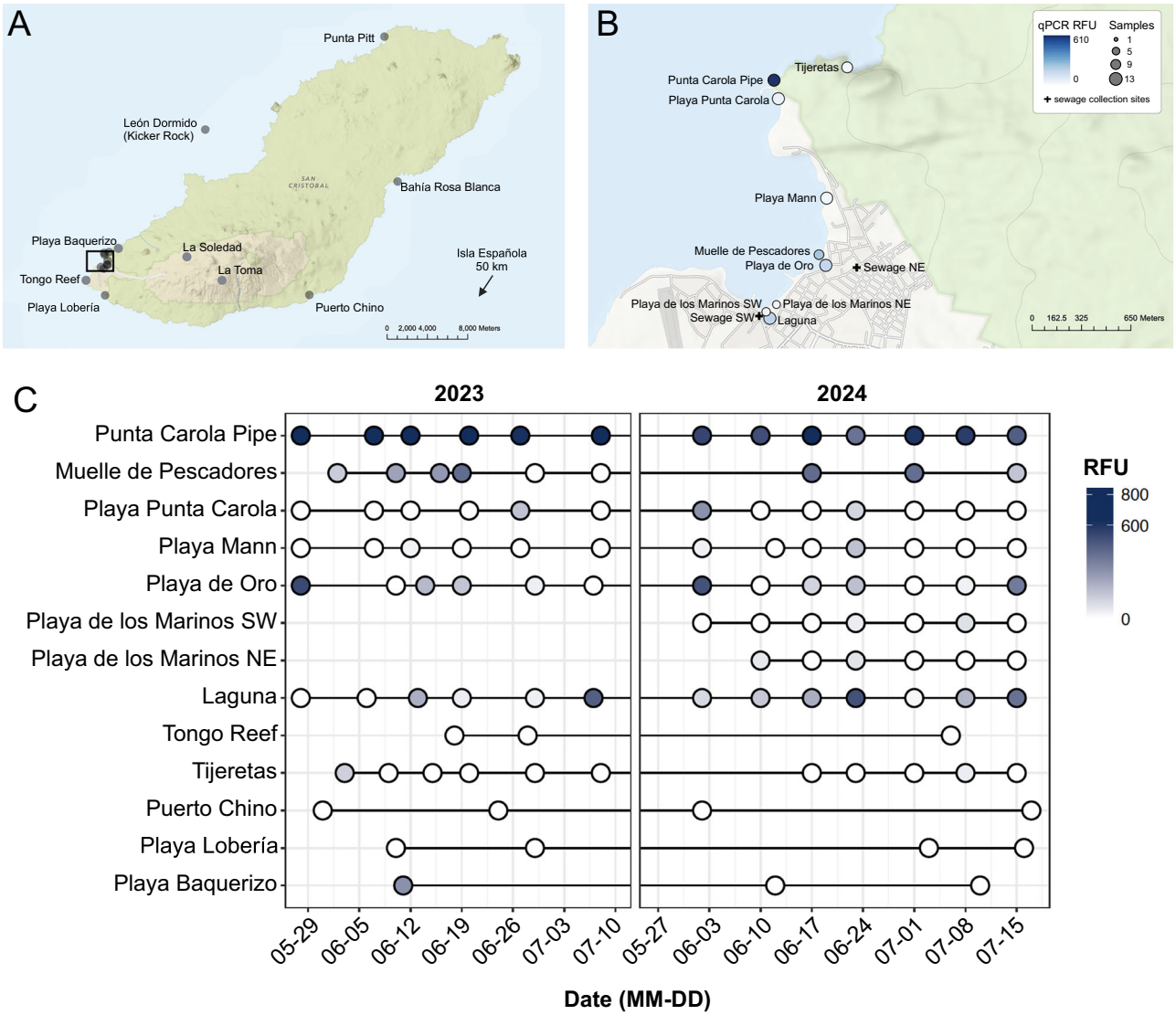

Fig. 2 | Identifying sites of wastewater contamination in the Galápagos marine ecosystem. A Map of San Cristóbal Island. Points indicate locations where water was collected and assayed for fecal contamination by qPCR. The box indicates the region shown in (**B**), where sampling was most intense, and which is centered on the Puerto Baquerizo Moreno, where population density and tourism are highest on the island. The color intensity of the dots indicates the relative fluorescent units (RFU) for the human stool qPCR assay, and the size indicates the number of samples collected over a 2-year period. **C** Dot plot showing relative fluorescent units (RFU) results for the human stool qPCR assay over a two-year period for 13 sites shown. Each point represents a single sampling event. Maps were created in ArcGIS software using the Esri Outdoor basemap. Detailed information and location data for sampling sites are provided in Supplementary Data 2.

occurs from the beach (Fig. 2B). In addition, the two sampling sites at Playa de los Marinos are separated from the Laguna by a small beach strip that likely prevents coliform movement during times of low precipitation.

Positive detection of human stool markers near populated areas raises concerns about contamination from untreated sewage. However, our qPCR assay detects DNA and thus cannot distinguish between viable and nonviable fecal bacteria. To assess bacterial viability at sites identified by qPCR testing, we quantified *E. coli* and coliforms directly from the same water samples analyzed by qPCR using MC-Media Pads, a miniaturized, dry culture system that enables colony-forming unit (CFU) enumeration without the need for media preparation (Fig. 1B). This analysis revealed >3000 CFU/mL of coliforms in the water around the Punta Carola Pipe and similarly high values in water from the Laguna site at most of the assayed time points (Supplementary Fig. 2). The other sites near the WWTP pumping stations, such as Muelle de Pescadores and Playa de Oro, also occasionally had counts >3000 CFU/mL. These findings indicate the presence of viable fecal indicator bacteria at sites where human-specific markers were detected. While *E. coli* and coliforms alone cannot distinguish between animal and human sources, the combination of our human-specific qPCR detection and concurrent recovery of viable coliforms suggests that the marine environment around Puerto Baquerizo Moreno is contaminated with human-derived waste.

Metagenomic sequencing identifies human fecal contaminants

Although our data highlight sites potentially contaminated with untreated sewage, these approaches do not reveal the broader impact on marine microbial diversity, nor enable a detailed view of microbial gene presence, such as AMR genes. Therefore, we conducted long-read metagenomic analysis of ten samples collected over the summers of 2022 and 2023. We sampled eight sites near Puerto Baquerizo Moreno and the broader archipelago, two of which were sampled in both years (Fig. 1C). Since sewage has been shown to reflect the enteric microbiome of resident human populations[23], we also directly sampled untreated wastewater at two sites within the municipal combined

sewage overflow system. Nanopore sequencing generated an average of 4.42×10^6 reads per sample, with a mean read length of 1460 bp (median N50 = 6197 bp), for an average yield of 12×10^9 bp per sample (Supplementary Data 3). Sites clustered predominantly into two groups based on taxonomic abundance of genera (Fig. 3A, top dendrogram). One group includes a remote beach (Playa Baquerizo), a distant uninhabited island (Española), a commonly used beach within city limits (Playa Mann), and the 2023 sample from the port's fishing pier (Muelle de Pescadores). Apart from the pier and Playa Mann, all sites are relatively remote, and the genera observed are characteristic of marine ecosystems, including cyanobacteria (*Synechococcus, Prochlorococcus*), eukaryotic phytoplankton (*Chaetoceros, Ostreococcus*), and heterotrophic marine bacteria (*Planktomarina, Pseudoalteromonas, Alteromonas, Vibrio, Sphingobacterium*). The relative paucity of enteric microbes detected at these sites suggests little or no exposure to untreated wastewater. Interestingly, the fact that one of the most central beaches (Playa Mann)—a site heavily visited by both locals and tourists—has a taxonomic profile similar to remote sites (Fig. 3A) and shows limited detection of human stool contamination by qPCR (Fig. 2B, C) suggests that recreational activity in and around the water is not sufficient as a source of fecal contamination.

The second cluster (Fig. 3A, top dendrogram) is comprised primarily of wastewater-associated sites, including the two sewage samples, the two sites known to be in proximity to untreated wastewater outfall (Punta Carola Pipe and Laguna), and the 2022 sample from the fishing pier (Muelle de Pescadores). A very different core set of genera predominates at these locations, including enteric (*Arcobacter, Bacteroides, Bifidobacterium, Clostridium, Escherichia, Streptococcus)* and environmental bacteria (*Pseudomonas, Acinetobacter)*. Many of the genera detected in these samples are potential pathogens of both humans and animals, and the presence of *Escherichia* indicates coliforms in the marine environment near wastewater outfall sites and, not surprisingly, the municipal sewage system. The similarity in taxonomic profiles between marine water near outfall sites and samples collected directly from the municipal sewage system, together with our qPCR (Fig. 2) and CFU results, strongly supports the conclusion that these locations are contaminated with untreated sewage.

A diverse resistome detected at wastewater-associated sites

Since human waste can be a source of AMR in the environment[24–26], we next sought to use our long-read metagenomic sequencing data to detect AMR genes at each site as a proxy for environmental antimicrobial resistomes. We observed a large and diverse set of AMR genes across our metagenomic samples, including 94 resistance genes spanning nine antimicrobial classes (Fig. 3B). The highest density of AMR genes was observed in contigs generated from sewage samples, followed by the Punta Carola outfall site, while other sites contained few or no AMR genes (Fig. 3C). Separation of the AMR gene density by resistance class highlights a clear pattern of similarity between the Punta Carola Pipe and the two sewage sites (Fig. 3D), including a relatively strong presence of tetracycline, beta-lactam, and macrolide AMR genes, among others. A lower but detectable level of AMR genes in similar classes was observed in the 2022 Muelle de Pescadores sample (but notably not the 2023 sample), along with the sampling of the Laguna. Taken together, these data raise the possibility that sites affected by wastewater contamination may also be sources of AMR in the environment.

AMR phenotyping of environmental coliforms

The presence of AMR genes does not necessarily reflect the actual ability to resist antimicrobials[27,28]. Therefore, we next set out to determine the AMR phenotype of bacteria recovered from the marine ecosystem around the island. For this analysis, we focused on lactose-fermenting *Enterobacteriaceae* because *Escherichia* was detected by metagenomic sequencing at all five wastewater-associated sites (Fig. 3A), they are easy to subculture from the MC-Media Pads, and they are potential pathogens of humans and animals. In total, 183 lactose-fermenting *Enterobacteriaceae* isolates, predominantly *E. coli*, were cultured directly from freshwater, ocean water, outfall sites, or untreated sewage (see "Methods") and subsequently assessed for AMR against a panel of twelve clinically relevant antibiotics using Kirby–Bauer disk diffusion assays (Supplementary Data 4). For every antibiotic examined, the proportion of isolates showing a resistant phenotype was similar between municipal sewage and marine sites near suspected or confirmed outfall of untreated wastewater (Fig. 4A). Streptomycin had the highest overall resistance (86 of 183; 47%), followed by Ampicillin (74 of 183 isolates; 40.4%).

MDR, defined as resistance to antibiotics from three or more different classes, was observed in only three isolates recovered from non-wastewater sites. In contrast, 26 of 68 isolates (38.2%) from marine sites near wastewater outfall and 35 of 84 (41.7%) sewage samples were MDR. Classifying all 183 isolates by their resistance profiles highlights 64 MDR isolates that gave rise to 50 unique resistance profiles (Fig. 4B, asterisks). While ampicillin and tetracycline resistance were present in most MDR isolates, the large number of unique MDR combinations hints at a potential genetic diversity that cannot be explained solely by the transmission of one or a few independent resistant lineages. Some sewage and outfall isolates are phenotypically resistant to six or more antibiotic classes. Taken together with our metagenomic data (Fig. 3), these results highlight a diverse and functional AMR landscape around the island. Finally, we observed three unique strains carrying phenotypic resistance to meropenem, which is notable given the classification of carbapenem-resistant *Enterobacterales* (including *E. coli*) as a critical priority bacterial pathogen by the WHO[29].

Phylogenomic analysis of antimicrobial-resistant *E. coli*

The presence of AMR—particularly MDR—in sewage, outfall, and to a lesser extent in ocean water around San Cristóbal prompted us to explore the genomic basis of these resistance phenotypes within *E. coli*. We selected 53 of the 183 lactose-fermenting *Enterobacteriaceae* isolates with AMR phenotypes (Fig. 4) for long-read sequencing, focusing primarily on MDR isolates (Supplementary Data 4). De novo assembled contigs were evaluated based on size and GC content, resulting in the removal of eight samples with potential poor quality (e.g., co-assemblies of multiple or non-*E. coli* genomes, incomplete sequences, etc.) (Supplementary Fig. 3 and Supplementary Data 5). Of the remaining 45 high-quality assemblies, all yielded complete, ungapped bacterial genomes, and 37 included at least one complete plasmid (Supplementary Data 5). Using these genomes and plasmids, we broadly classified our *E. coli* into clades based on Clermont typing[30] and multi-locus sequence typing (MLST)[31]. This analysis identified five distinct phylogroups in our study, including: 21 group A isolates (commensals associated human and animal colon); 15 group B1 isolates (environment- and animal-associated); one group B2 isolate (highly virulent, human-associated); five group D isolates (more virulent, extraintestinal pathogen); two group E isolates (related to D and associated with foodborne outbreaks but can be commensal); and one group G isolate (similar to B2, human- and animal-associated, potential zoonotic transmission) (Fig. 5). Notably, our analysis identified several globally distributed, high-risk pandemic clones associated with MDR, including ST10, ST58, ST69, and ST155 (Fig. 5)[32].

To complement our phylogenetic analysis and link AMR phenotypes to genes, we annotated AMR genes on all isolated chromosomes and plasmids (see "Methods") (Fig. 5). These analyses identified multiple genes and operons, including multidrug efflux genes and quinolone resistance genes such as *acr(E/F/S)*, *mdt(E/F/H/M/N/O/P)*, *emr(E/R)*, and *evg(A/S)*, that were present on the chromosome of nearly every isolate examined and rarely, if ever, detected on plasmids (Fig. 5, top, stars). Aside from these examples, most AMR genes we identified were

https://doi.org/10.1038/s41467-026-74899-9

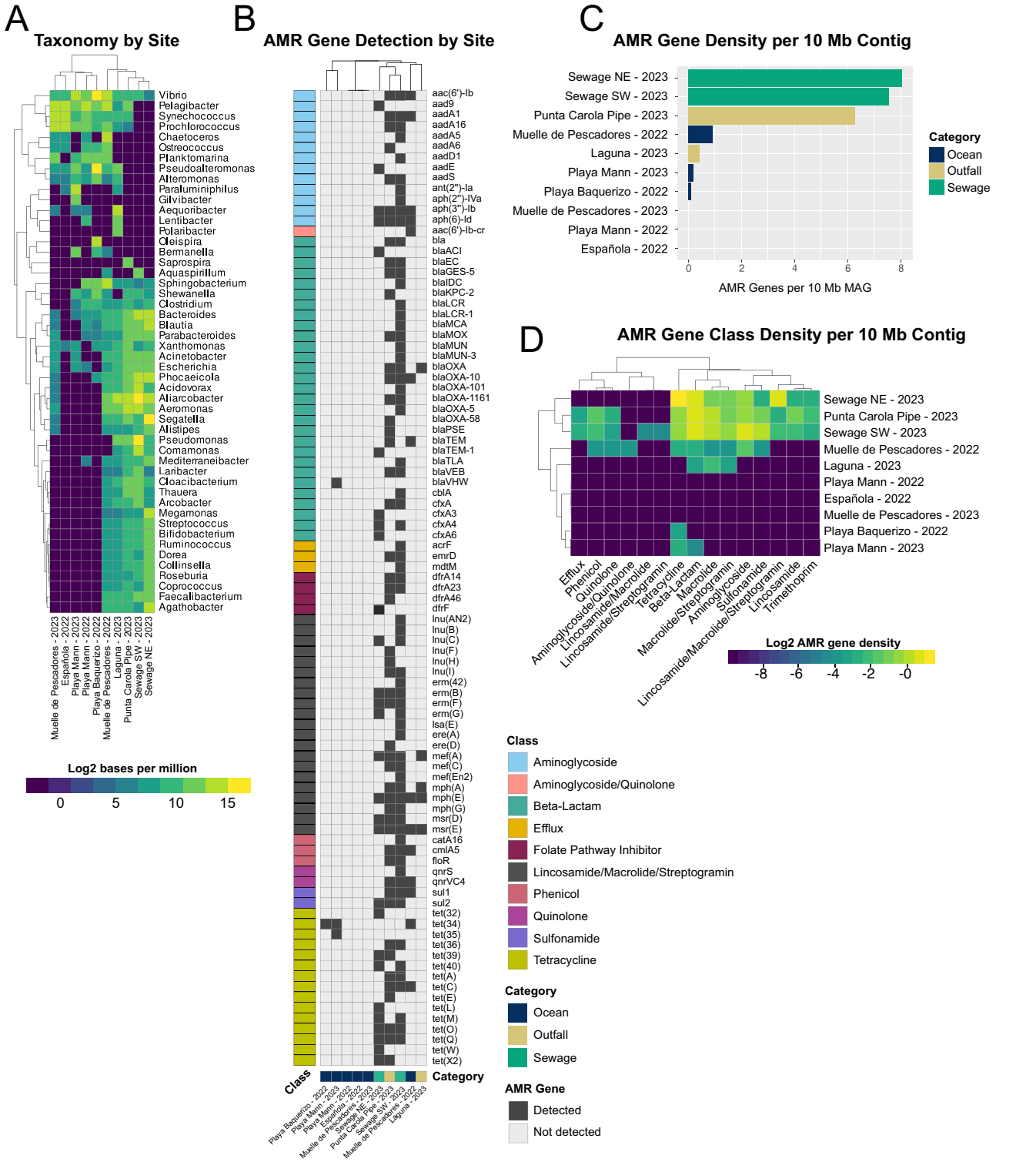

Fig. 3 | Wastewater contamination remodels the marine microbiome and gives rise to a diverse antimicrobial resistome. A Heatmap showing relative taxonomic abundance (Log2 bases per million) at the genus level for bacteria and archaea in water and sewage metagenome samples, as classified by the CZ ID tool[58]. Only taxa with >85% nucleotide identity and >500 bp alignment length are included. The top 50 most abundant taxa are shown. **B** Presence/absence results for specific antimicrobial resistance (AMR) genes detected in contigs >500 bp using AMRFinderPlus[61]. Columns are clustered by average linkage hierarchical clustering using Jaccard distances. Colors to the left and below indicate AMR gene class and sampling site category, respectively. The total AMR gene density (**C**), and the AMR density broken down by AMR gene resistance class (**D**) are displayed as the number of AMR genes per 10 Mb of assembled contig length.

https://doi.org/10.1038/s41467-026-74899-9

A

Site Category	Isolates n	MDR n (%)[†]	Resistant and Intermediate Isolates, n (%)											
			AMC30	AMP10	FOX30	CRO30	MEM10	CN10	S10	AZM15	C30	CIP5	TE30	SXT25
Fresh Water	12	0 (0.0)	1 (8.3)	3 (25.0)	0 (0.0)	0 (0.0)	0 (0.0)	0 (0.0)	1 (8.3)	2 (16.7)	0 (0.0)	0 (0.0)	1 (8.3)	0 (0.0)
Ocean Water	19	3 (15.8)	3 (15.8)	9 (47.4)	1 (5.3)	0 (0.0)	0 (0.0)	0 (0.0)	6 (31.6)	2 (10.5)	0 (0.0)	4 (21.1)	1 (5.3)	3 (15.8)
Outfall	68	26 (38.2)	19 (27.9)	26 (38.2)	3 (4.4)	6 (8.8)	1 (1.5)	7 (10.3)	37 (54.4)	19 (27.9)	10 (14.7)	13 (19.1)	29 (42.6)	18 (26.5)
Sewage	84	35 (41.7)	19 (22.6)	36 (42.9)	10 (11.9)	6 (7.1)	2 (2.4)	8 (9.5)	42 (50.0)	41 (48.8)	8 (9.5)	18 (21.4)	29 (34.5)	19 (22.6)

[†] Defined as non-susceptibility to ≥1 agent in ≥3 antimicrobial categories.

B

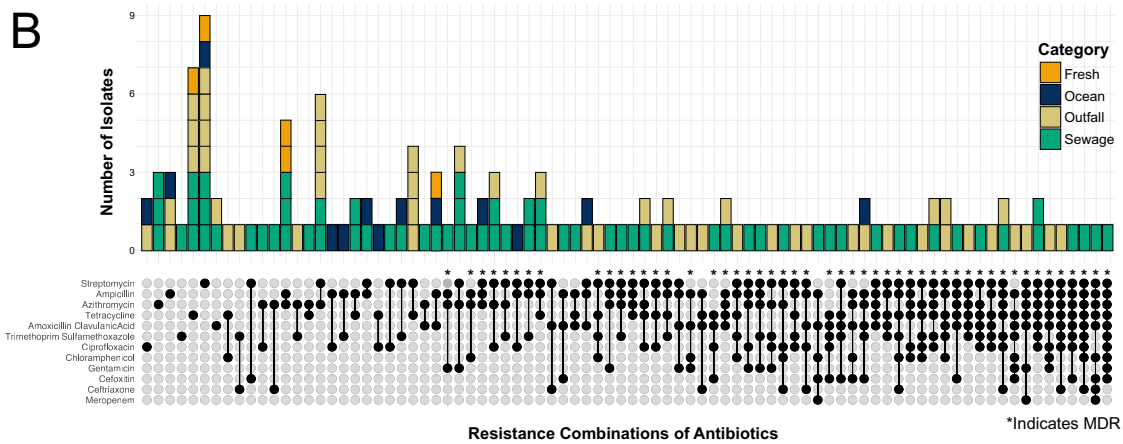

Fig. 4 | Phenotypically diverse MDR *E. coli* are present in sewage and marine sites near wastewater outfall. A Table showing counts of lactose-fermenting *Enterobacteriaceae* isolates exhibiting non-susceptibility to antibiotics, as assessed through standardized Kirby–Bauer disk diffusion assays, separated by site classification of freshwater, ocean water, outfall, or sewage. Multidrug-resistant (MDR) counts are defined as resistance to three or more different antibiotic classes. Beta-lactams are grouped together in the table, and rows are sorted by the number of isolates. Antibiotic classes are abbreviated as follows: AMC amoxycillin/clavulanic acid, AMP ampicillin, AZM azithromycin, C chloramphenicol, CIP ciprofloxacin, CN gentamicin, CRO ceftriaxone, FOX cefoxitin, MEM meropenem, S streptomycin, SXT trimethoprim-sulfamethoxazole, TE tetracycline. **B** Stacked bar chart (top) and "Upset" plot (bottom) showing the number of isolates and site categories for different antibiotic resistance combinations. Asterisks indicate AMR combinations that meet the criteria for being MDR.

either never or only rarely found on the chromosome but instead were localized to a bacterial plasmid. For example, AMR genes belonging to aminoglycoside, tetracycline, sulfonamide, or macrolide classes were almost exclusively plasmid localized (Fig. 5, top), thus highlighting the importance of long-read sequencing and de novo plasmid assembly for AMR gene discovery. Our analysis also identified a subset of phylogenetically related MDR isolates (PCP07014, SW070912, SW070910, SW071620, and PCP06238) as phylogroup D, suggesting that these isolates may be particularly concerning because of their potential to cause extraintestinal infections and to resist multiple classes of antimicrobials (Fig. 5, left, red text). Consistent with this notion, three of these isolates were identified by MLST analysis as belonging to the ST69 complex (Fig. 5), a global pandemic *E. coli* lineage commonly associated with extraintestinal infections[33], including urinary tract infections[34]. Interestingly, all phylogroup D isolates were from sewage (SW070912, SW070910, SW071620) or isolated from the marine environment near the Punta Carola outfall site (PCP07014, PCP06238), and all were isolated within the same three-week period (Supplementary Data 4), thus directly implicating wastewater contamination in the emergence of MDR in the marine environment. Finally, four of these isolates exhibited similar resistance profiles and plasmid-associated AMR gene content, via the disk diffusion assay and whole-genome sequencing, respectively (Fig. 5), linking MDR phenotypes to specific AMR gene assemblages on plasmids.

Strain-level analysis of phylogroup D *E. coli*

Given their pathogenic potential and large AMR burden, we turned our attention to the phylogroup D *E. coli* isolates SW070912, SW070910, SW071620, PCP07014, and PCP06238 and carried out a pangenome analysis to explore relatedness of these strains beyond analysis of single copy genes (Fig. 6A). The pangenome consisted of 3483 core gene clusters and an accessory genome comprised of 1354 gene clusters across the five isolates (Fig. 6A). Our pangenome analysis showed that all five strains were closely related, with core genomes that differed by no more than 300 SNPs between any two isolates. Two MDR strains (SW070910 and SW071620) isolated one week apart from the same municipal wastewater system shared a nearly identical core and accessory genome (the former differing by only 150 SNPs) (Fig. 6A). Interestingly, whole-genome alignment showed that the two genomes were colinear apart from a 469 Kb region in SW070910 that is inverted relative to SW071620 (Supplementary Fig. 4). The highly conserved nature of their chromosomes, along with their nearly identical AMR genotypes and phenotypes (Fig. 5), suggests that these two strains share recent common ancestry.

Our observation that *E. coli* isolates SW070910 and SW071620 are nearly genetically identical, together with previous reports that *E. coli* preferentially transfer plasmids to closely related "kin"[35], prompted us to compare the plasmid content of these two *E. coli* strains. SW070910 and SW071620 yielded four and five full-length plasmids (P1-5), respectively (Fig. 6B and Supplementary Data 5). Conjugative plasmids P4 from SW071620 and P2 from SW070910 were similar in length and highly syntenic (Fig. 6C), indicating a shared evolutionary origin. Interestingly, the mobilizable plasmid P1 from strain SW071620 is fully syntenic over its 107 kb length with plasmid P1 from strain SW070910, a conjugative mega-plasmid over 200 kb in length (Fig. 6C and Supplementary Data 5). In addition, conjugative plasmid P3 from strain SW071620 is partially syntenic with SW070910 P1, aligning over ~50 kb of its 67 kb length (Fig. 6C and Supplementary Data 5). Together, these results suggest that these plasmids may be undergoing fusion and/or

https://doi.org/10.1038/s41467-026-74899-9

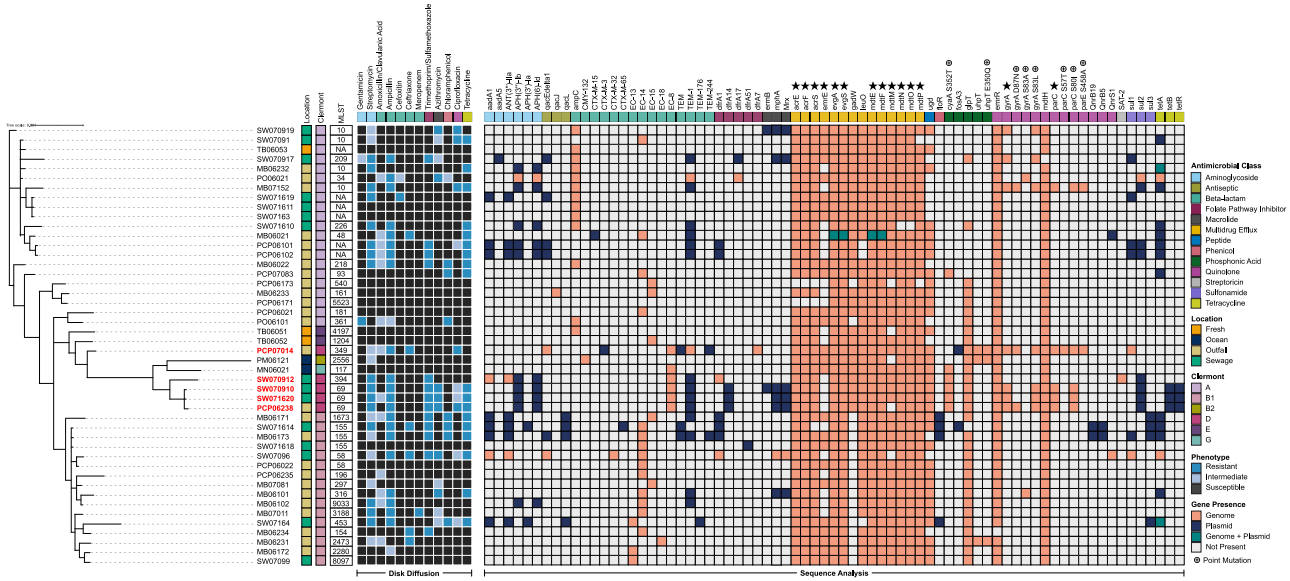

Fig. 5 | Integrating AMR phenotypes and genotypes of MDR *E. coli*. Visualization showing AMR genes (top) detected in either the genome (pink) or plasmid (dark blue) or both (green) for 45 *E. coli* isolates (left). White cells indicate no AMR gene detected. Isolates were clustered based on single-copy genes (phylogenetic tree) and grouped by class of AMR (top; color). Kirby–Bauer disk diffusion assay results are shown (dark heatmap, left). Stars indicate AMR genes observed mainly in the genome (top). Circled cross symbol (top) indicates AMR genes with point mutations. Red identifiers (left) indicate MDR Clermont D group *E. coli* isolates are described in more detail in Fig. 6.

fission in different bacterial strains, resulting in within-strain plasmid heterogeneity.

To assess whether this plasmid 'shuffling' may contribute to AMR gene diversity in our study, we compared the mega-plasmid and two smaller syntenic plasmids to a database of plasmid sequences spanning 40,757 globally distributed plasmids with significant counts of Enterobacteriaceae-origin plasmids[36]. Each plasmid was compared to the database via BLAST, and database "hits" were used to construct a correlation matrix heatmap (Supplementary Fig. 5 and "Methods"). The color of each grid in the heatmap represents the extent to which two regions of the same plasmid (*X*- and *Y* axis) shared a common set of database hits (calculated as a Jaccard similarity) (Supplementary Fig. 5). This visualization reveals conserved plasmid insertions (solid dark red triangles) of varying size as well as novel insertions not seen across the entire database (light stripes extending fully or partially across the heatmaps) (Supplementary Fig. 5). Annotating our correlation heatmaps with the location of AMR genes places resistance in the context of the conservation landscape for each plasmid. For example, except for a few small regions, a contiguous three-quarters of plasmid P3 from SW071620 is observed within the database (Fig. 6D, right, arrow), representing an example of a stable plasmid "backbone" in a plasmid devoid of AMR genes. Similarly, P1 from SW071620 contains a ~20 kb conserved insertion (Fig. 6D, middle, arrow), with AMR genes found in either very small areas of conservation or areas of poor conservation, suggesting a recent acquisition of these genes into a plasmid backbone. The localization of AMR genes in areas of limited or poor conservation becomes more apparent in the mega-plasmid (Fig. 6D, left), whose AMR genes fall in regions of the plasmid that are neither commonly associated with the general backbone of the plasmid nor with other genetic regions carrying AMR genes. This suggests that AMR gene combinations leading to MDR were formed in plasmids without being linked to fully conserved cassettes or stable plasmid backbone lineages. Since bacteria carrying these plasmids were isolated from municipal wastewater with access to the marine environment, these plasmids have the potential lead to infections with pathogenic *E. coli* that are refractory for antimicrobial treatment and therefore have the potential to cause significant morbidity and mortality in animals or humans.

Discussion

The Galápagos Islands, a UNESCO World Heritage Site, are cherished for being among the most biologically unique and ecologically fragile ecosystems on Earth. Although 97% of the land and 100% of the surrounding waters are protected within the Galápagos National Park (Parque Nacional Galápagos), the islands support a rapidly growing resident population and face substantial tourism pressure, with ~29,000 residents and 270,000 visitors in 2022. In San Cristóbal, this has placed a significant strain on the municipal WWTP, a combined sewer overflow system that is prone to overflow and often releases untreated wastewater into the waters surrounding the island's city of Puerto Baquerizo Moreno[20]. Effective wastewater management is critical to the health of island residents, and we initiated this study in response to community concerns about the effects of untreated wastewater on human and environmental health. To address these concerns, we developed a multimodal mobile microbiological laboratory (Fig. 1). Using this platform, we identified marine sites contaminated with human fecal bacteria (Fig. 2). Long-read metagenomic sequencing of these sites reveals fundamental shifts in marine microbial community composition and the presence of numerous AMR genes (Fig. 3). Finally, analysis of lactose-fermenting *Enterobacteriaceae* isolates collected directly from sewage or marine waters highlights numerous MDR phenotypes (Figs. 4 and 5), with evidence of plasmid sharing and recombination among distinct *E. coli* strains (Fig. 6).

Puerto Baquerizo Moreno's WWTP is designed with three pumping stations. However, frequent mechanical failures result in the discharge of untreated wastewater into either the Punta Carola Pipe or through two excess-flow drains at Playa de Oro and Laguna/Playa de los Marinos. These sites, along with Muelle de Pescadores, exhibit high levels of coliform growth (Supplementary Fig. 1) and strong human fecal bacteria qPCR signal (Fig. 2C), with differential temporal patterns of contamination. These differences may be influenced by factors such as changing currents, weather patterns[37], animal migration, or sewage release[19]. Importantly, although none of our coliform assays are approved for informing public health recommendations, a conservative interpretation of the results would still signal significant concern to human health. Tests conducted by local authorities in November 2024, just four months after our last round of testing

https://doi.org/10.1038/s41467-026-74899-9

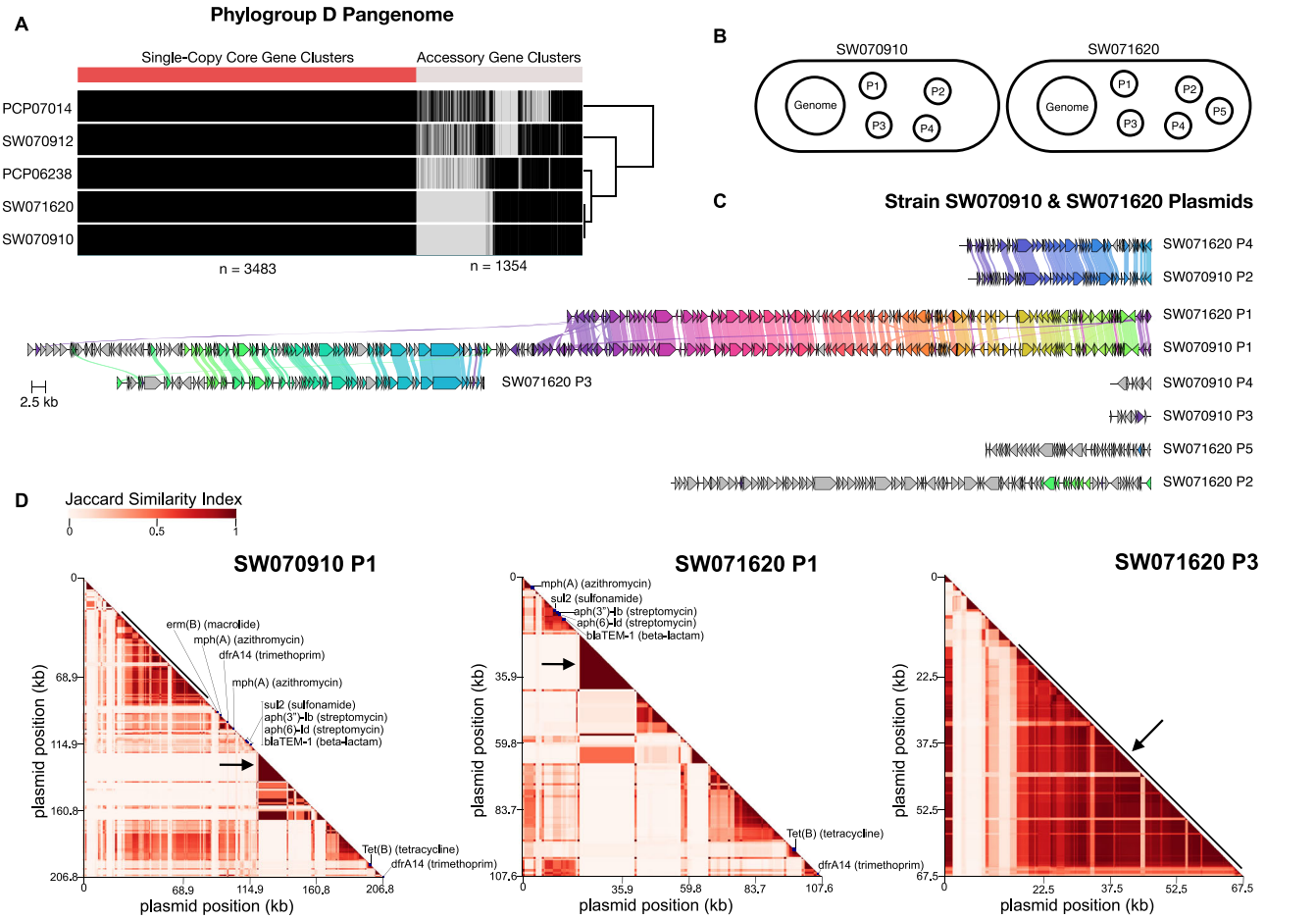

Fig. 6 | Strain-level analysis of phylogroup D *E. coli* identifies dynamic plasmid sequences containing AMR genes. A Schematic of strains SW070910 and SW07620. Strain SW070190 contains four plasmids (P1-P4) and strain SW071620 contains five plasmids (P1-P5). **B** Single-Copy Core Gene Cluster (SCG) analysis of all phylogroup D genomes from this manuscript using anvi'o. The genomes of strains SW070910 and SW07620 are highly conserved, with nearly identical SCG and accessory genes. **C** Synteny plots of plasmids from strains SW070910 and SW07620. Plasmids are labeled in descending size order (P1 = largest, P2 = second largest, etc.). The code for generating these images is available in the GitHub repository for this manuscript. **D** Correlation heatmap for *E. coli* plasmid P1 from strain SW070910 and plasmids P1 and P3 from strain SW071620. Heatmap color intensity reflects Jaccard Similarity Index. See Supplementary Fig. 5 for details on interpretation of correlation heatmaps.

(Fig. 2C), identified potentially dangerous levels of fecal coliforms and led the Galápagos National Park to temporarily restrict access to Playa del los Marinos and Playa de Oro[38], the latter of which was also seen in our study to have relatively high levels of contamination on multiple occasions in 2023 and 2024, and as recently as July 2024 (Fig. 2C). Our results provide context for this policy decision and pinpoint specific locations, sources, and surveillance tools to monitor and intervene to minimize the threat of AMR bacteria to the biodiversity of this delicate ecosystem. Ultimately, this will require a renewed effort to modernize wastewater infrastructure on the island.

Genomic surveillance of AMR is critical for informing how and when resistance phenotypes may develop and spread across human, animal, and environmental systems[39]. Even though our long-read metagenomic sequencing was more shallow than standard laboratory-based short read sequencing, it proved sufficient for genus-level resolution and AMR gene detection (Fig. 3). Using our mobile qPCR platform (Fig. 2) to guide our metagenomic sequencing identified sites where the normal marine microbiome had been dramatically remodeled by wastewater contamination, introducing bacterial pathogens such as *Streptococcus*, *Bifidobacterium*, *Arcobacter*, *Pseudomonas, Clostridium, Bacteroides, Acinetobacter*, and *Escherichia*. The Galápagos is home to large populations of sea lions (*Zalophus wollebaeki*), and San Cristóbal in particular has some of the highest concentrations of sea lions in all of the archipelago[40], with multiple rookeries (breeding grounds) and haulouts (resting areas) for this endangered species intermixed with tourist beaches, resulting in many close human-animal interactions[41]. Consequently, there is a high potential for the wastewater-associated strains described in this study to colonize sea lions, leading not only to disease but also to further dispersal of AMR in the marine environment. *E. coli* is the most common bacterium associated with superficial wounds, skin abscesses, and ocular lesions in sea lions[42] and has been linked to endocarditis[43]. Notably, higher rates of *E. coli* colonization and increased prevalence of AMR in sea lions have been linked to proximity to humans[44,45]. The intense tourism pressure and close intermixing of humans and sea lions on San Cristóbal raises the possibility that marine mammals could be at risk of exposure to MDR *E. coli*, underscoring the importance of viewing AMR as a One Health challenge, rather than simply a human health threat.

We observed a significant AMR burden in our lactose-fermenting *Enterobacteriaceae* isolates, with 64 of the 183 isolates exhibiting 50 unique MDR phenotypes. Notably, this included three isolates that were resistant to meropenem, a "last resort" carbapenem antibiotic (Figs. 4 and 5). The wide variety of MDR profiles in our data suggests that AMR in the Galápagos may be highly dynamic, with frequent gains and losses of AMR genes potentially driven by reassortment and recombination events. Consistent with this notion, our comparative

genomic analysis of plasmids from MDR *E. coli* showed that AMR genes appear to be subject to frequent 'shuffling' within plasmid backbones (Fig. 6 and Supplementary Fig. 5). One interpretation of these data is that MDR in our *E. coli* isolates arises from recent genomic changes within plasmids rather than simply through acquisition of extant MDR-conferring plasmids or other genomic cassettes. Therefore, plasmid rearrangement/recombination offers one mechanism to explain much of the diversity and novelty of MDR phenotypes in the Galápagos (Fig. 4B). The reassortment of genomic regions to generate novel MDR phenotypes in highly mobile plasmids could introduce MDR into pathogenic bacteria, ultimately leading to human or animal disease.

Although *E. coli* is most commonly associated with the lower gastrointestinal tract of mammals, it can also persist and even become naturalized in extraintestinal environments[46]. Coastal marine sediment has been shown to be a reservoir for *E. coli* and a potential source of bacterial persistence and reemergence in the environment[47]. Once in the environment, AMR can spread rapidly. For example, within three months of the discovery of *mcr-1*, a plasmid-mediated colistin-resistance gene in Gram-negative organisms, it was detected in organisms in more than 20 countries[48]. In Latin America and the Caribbean, *E. coli* accounts for the largest pathogen-attributable fraction of human deaths associated with bacterial AMR[49]. This is of particular importance given our detection of multiple pandemic-associated *E. coli* strains, including ST10, ST58, ST69, and ST155 (Fig. 5). Curtailing the spread of AMR across ecosystems is vital to One Health but will require a deeper understanding of the mechanisms that lead to the emergence of AMR strains and plasmids in complex microbial environments. Recent work on the healthcare-associated AMR plasmid pOXA-48 has shown that horizontal transmission efficiencies can vary by orders of magnitude across bacterial strains[50]. Using a population dynamics model, the authors went on to show that a single successful association of a plasmid with a bacterial host was sufficient for establishment and stable maintenance in a complex microbial community and, ultimately, resistance to a broad range of antibiotic concentrations[50]. Similar experimental and modeling approaches with a focus on environmental—rather than gut-associated—microbiomes could help elucidate key factors that allow the dissemination of wastewater MDR plasmids through marine ecosystems.

Our mobile AMR lab is not without limitations, and there are several opportunities for improvement. First, the portable qPCR and Oxford Nanopore sequencing instruments are relatively expensive, and consumables for portable assays tend to be more costly than their lab-based counterparts (Supplementary Data 1). However, all equipment and assays used in this study are well-suited for traditional bench-based research as well, meaning that any capital investment in these technologies does not restrict one to field-based work or even AMR work, for that matter, which means that equipment could be used for other purposes. Second, although the use of MC-Media pads greatly reduces the need for petri dishes and solid agar, our culture work still relies on MacConkey and Mueller-Hinton agar plates for *Enterobacteriaceae* isolation and Kirby–Bauer disk assays, respectively (Fig. 1B). Without access to an autoclave on site, these plates constituted our single largest logistical challenge in terms of storage and transport. An alternative approach, such as a "Redigel" system, where pectin-based liquid media is poured on-site into dishes pre-coated with divalent cation salts, could be used in place of MacConkey agar plates[51]. In addition, minimum inhibitory concentration (MIC) assays using a "Sensititre" system, in which antibiotics are dehydrated on microtiter plates, could be an alternative to Kirby–Bauer disk assays, allowing for room-temperature storage and less plastic waste. Third, bioinformatic analysis of sequencing data was not carried out on-site and remains a major bottleneck to getting rapid insights from portable sequencing. Portable external graphical processing units (GPU; e.g., NVIDIA DGX Spark) together with GPU-optimized workflows[52] would allow demultiplexing, basecalling, and accelerated downstream analyses on-site using only a laptop. Finally, although not explored in this study, additional capabilities of nanopore sequencing such as base modification detection and selective or "adaptive" sequencing[53–55] could be used for more detailed characterization of MDR strains and more sensitive detection of large panels of AMR genes, respectively.

AMR is a global threat that will require creative solutions in areas of the world where access to modern laboratory infrastructure and resources is limited. Despite the clear threat that AMR poses to humans and animals, relatively little effort has been devoted to optimizing environmental AMR surveillance methods in LMICs, where socioeconomic factors can drive the rapid emergence of MDR organisms. Just as mobile surveillance efforts helped track Zika virus evolution in Brazil[56] and decentralized sequencing proved vital for SARS-CoV-2 surveillance in Africa[57], the approaches we outlined here provide a robust framework for community-driven AMR research in low-resource areas. Our use of portable, smartphone-powered qPCR technology, ready-to-use lyophilized qPCR reactions (Biomeme), and MC-Media pads for isolating bacteria eliminates time-consuming and error-prone procedural steps, reducing the need for skilled technicians and opening the door to engaging local stakeholders in the surveillance work. Our discovery of numerous *E. coli* MDR phenotypes and a diverse and dynamic resistome landscape in the Galápagos only further highlights the importance of environmental monitoring of AMR, especially given the rapid dissemination of plasmid-encoded AMR genes. Mobile microbiology laboratories offer a strong model for global AMR surveillance to inform policy, public works, and clinical decision-making.

Methods

Sampling of wastewater, marine, and freshwater sources

Marine and freshwater samples were collected using sterile 210 mL Whirl-Pak bags (Whirl-Pak Filtration Group). Wastewater samples were collected using organic cotton tampons free of antimicrobials, fragrances, deodorants, and chlorine-whiteners (7th Generation). Briefly, tampons were suspended individually from a string, lowered into the wastewater stream, and allowed to passively sample for one minute. The swab was recovered, sealed in a plastic bag, and liquid was extruded from the swab by compressing the bag by hand, and the corner of the bag was cut to recover the liquid sample into a 50-ml conical centrifuge tube. Each sample's collection time and geolocation were recorded using metadata from cell phone photographs taken at the time of collection. GPS data was overlayed onto maps created using ArcGIS software and the Esri Outdoor basemap, which uses the following data sources: Esri, TomTom, Garmin, FAO, NOAA, USGS, OpenStreetMap contributors, and the GIS User Community. Samples were either processed immediately or stored at 4 °C for ≤5 h before processing.

Water sample processing and mobile multiplexed qPCR

In total, 200 mL of each water sample was filtered through a 0.2-μm nitrocellulose filter in a 100 mL disposable analytical filter funnel (Nalgene) using a Mini LABOPORT N96 vacuum pump (KNF) or a hand-operated vacuum pump (Nalgene). Nitrocellulose membranes were recovered from filter funnels and placed in a Biomeme 5-mL sample homogenization tube containing a 0.5-inch steel ball bearing and 2 mL of lysis buffer. Membrane contents were lysed by vigorous hand shaking for 1 minute. DNA was then extracted from 1 mL of homogenate using the M1 Sample Prep Cartridge Kit for High Concentration DNA (DNA-HI), per the manufacturer's instructions (Biomeme). DNA was used immediately or stored at −20 °C until use. To detect relative levels of human and animal fecal contamination, 20 μL of DNA was added to BioPoo Enterococcus Panel PCR Go-Strips (Biomeme), and qPCR was run on a Franklin "Three9" thermocycler (Biomeme) controlled using the Biomeme Go app (v2.1.1) on a smartphone. The BioPoo assay is a triplex probe-based qPCR assay that simultaneously

detects the following targets in each sample: (1) pan-stool marker, *Enterococcus faecalis* with probe conjugated to 6-carboxyfluorescein (FAM); (2) human-specific fecal marker, HF183 *Bacteroides* 16S rRNA with probe conjugated to Texas Red; and (3) Internal positive control (IPC) conjugated to cyanine5 (Cy5). Samples were considered positive if the CT value was less than 38. Freshly opened bottled drinking water was processed alongside ocean water and freshwater samples as a qPCR negative control. Step-by-step Standard Operating Procedures (SOPs) are available online for all aspects of our field-based mobile AMR lab (https://protocols.hostmicrobe.org/field-amr-sops).

Metagenomic sequencing with Oxford Nanopore Technologies (ONT)

Biomass was concentrated from sewage, outfall, and ocean water samples on 0.2-µm nitrocellulose filters as described above. The volume of liquid processed varied based on the biomass of the sample type: 10 ml for sewage, 200 ml for outfall sites, and 2 L for ocean water. DNA was extracted from filters using the DNeasy PowerSoil Pro Kit (Qiagen) with a modified preprocessing step. Briefly, filters were placed in a Biomeme 5 mL sample homogenization tube containing a 0.5-inch steel ball bearing and 2 ml CD1 buffer. Tubes were shaken by hand for one minute, and 800 µl of the homogenate was subsequently transferred to a PowerBead Pro tube. The remainder of the extraction proceeded per the manufacturer's protocol. DNA was quantified using the Qubit dsDNA High Sensitivity Assay Kit (Thermo Scientific) and was used immediately or stored at −20 °C. Sequencing libraries were prepared from 1 µg DNA using the Ligation Sequencing gDNA Kit (SQK-LSK110, Oxford Nanopore) with Solid Phase Reversible Immobilization (SPRI) beads. Libraries were sequenced with an Oxford Nanopore MinION using R9.4.1 flow cells.

Analysis of ONT metagenomic data

Metagenomic long-read data were basecalled using Dorado v0.3.1 using the super accuracy model (dna_r9.4.1_e8_sup@v3.6). The resulting fastq files were uploaded to the CZ ID online portal for long-read metagenomic analysis[58]. Results were filtered based on nucleotide alignment length >500, nucleotide percent identity >85%, and nucleotide bases per million >50. For AMR gene prediction, metagenomic data were processed as follows. Nanopore adapters were removed from reads with porechop (version 0.2.4), reads were quality filtered using filtlong (version 0.2.1), high-quality reads were assembled using Flye (version 2.9.5-b1801)[59] with the meta flag, assemblies were polished with three rounds of racon (version 1.5.0) and two rounds of medaka (version 1.8.0), frameshifts were corrected using proovframe (version 0.9.7)[60], and AMR genes were identified in contigs using AMRFinderPlus (version 4.0.19 with database version 2024-12-18.7)[61]. Heatmaps were generated in R. While sample volumes used as input for metagenomic sequencing varied between marine water, outfall, and sewage samples (see above), we do not anticipate issues in comparing results between sample types. Metagenomic libraries were normalized by DNA input and sequencing depth, mitigating the impact of disparate starting volumes on AMR gene quantification. However, we acknowledge that lower sequencing depths—particularly with Nanopore—may limit the detection of low-abundance genes.

Fecal coliform and *E. coli* culture

In all, 1 mL of each sample was added to an MC-Media Pad *E. coli* and Coliform test (Sigma) and incubated for 18–24 h at 37 °C. The next day, colonies of *E. coli* and other coliforms were counted by hand. Samples with growth too dense to be counted were diluted 1:10 (outfall) or 1:1000 (sewage) in sterile saline solution (Sigma) and re-cultured on a new MC-Media Pad. Up to five *E. coli* colonies per MC-Media Pad were subcultured on MacConkey II agar plates (Becton Dickinson) and incubated for 24 h at 37 °C for purity testing. Lactose-fermenting isolates were selected from MacConkey II plates with a sterile inoculation loop (Fisher Scientific) and suspended in 2 mL of sterile saline for antimicrobial susceptibility testing. The same inoculation loop was then submerged in 1 mL of LB broth, and the broth was incubated overnight at 35 °C and 1000 rpm on a BioShake iQ thermomixer (QInstruments). Pellets from LB overnight cultures were stored at −20 °C for DNA extraction and sequencing.

Antimicrobial susceptibility testing

Kirby–Bauer disk diffusion assays were conducted to assess the antibiotic susceptibility of each isolate. Briefly, lactose-fermenting *Enterobacteriaceae* isolates or *E. coli* control strains ATCC 35218 and ATCC 25922 were visually adjusted to a 0.5 McFarland Standard (Hardy Diagnostics) in sterile saline solution. A sterile cotton-tipped applicator was then used to swab the bacterial suspension three times over the surface of two Mueller-Hinton II agar plates (Becton Dickinson) that had undergone manufacturer quality control analysis. After drying, six 6 mm antibiotic disks (Troy Biologicals) were pressed onto the surface of each plate. Twelve antibiotics were tested with each isolate: amoxicillin/clavulanic acid (20/10 mcg), azithromycin (15 mcg), cefoxitin (30 mcg), ceftriaxone (30 mcg), gentamicin (10 mcg), chloramphenicol (30 mcg), ampicillin (10 mcg), meropenem (10 mcg), streptomycin (10 mcg), tetracycline (30 mcg), sulfamethoxazole/trimethoprim (23.27/1.25 mcg), and ciprofloxacin (5 mcg). The zone diameters of clearance around each antibiotic disk were measured to the nearest millimeter after the plates were incubated at 37 °C for 16–20 h. When the full diameter could not be recorded (e.g., due to proximity to the plate edge), radii were recorded and doubled. For all antibiotics except for azithromycin, results were interpreted using zone diameter breakpoints (susceptible, intermediate, and resistant) according to the Clinical and Laboratory Standards Institute (CLSI) M100 standard[62]. Azithromycin was defined as wild-type or non-wild-type according to the CLSI M100 standard[62]. Since samples were selectively diluted to avoid over-plating and achieve countable colonies (see above), these data represent a qualitative snapshot of AMR profiles within *Enterobacteriaceae* rather than an absolute quantification of organism density or total AMR burden across sites.

Whole-genome sequencing and analysis of *E. coli* isolates

Pelleted lactose-fermenting *Enterobacteriaceae* isolates were resuspended in residual LB broth, and DNA was extracted using the DNeasy PowerSoil Pro Kit (Qiagen) and quantified using the Qubit dsDNA High Sensitivity Assay Kit (Thermo Scientific). DNA was used immediately or stored at −20 °C. Sequencing libraries were prepared from 400 ng DNA using the Native Barcoding Kit 24 V14 (SQK-NBD114.24, Oxford Nanopore). DNA was quantified after every step, and samples were normalized and pooled to equal concentrations for sequencing. Libraries were sequenced with an Oxford Nanopore MinION using R10.4.1 flow cells. Raw reads in POD5 format were basecalled using the Super Accuracy preset and demultiplexed using Dorado (version 0.9.6).

For analysis of isolate genomes, basecalled reads in fastq format were assembled with Autocycler (version 0.2.1)[63] using flye (version 2.9.5-b1801)[59], miniasm (version 0.3-r179)[64], and raven (version 1.8.3)[65] assemblers. Assembled contigs were re-oriented to the origin of replication with dnaapler (version 1.0.1). Anvio (version 8)[66] was used to annotate each genome and construct a genome database for all isolates. Single copy genes (SCGs) were obtained using the anvi-get-sequences-for-hmm-hits function in Anvio using the Bacteria_71 set of SCGs. SCGs were then used to construct a phylogenetic tree with MrBayes (version 3.2.7)[67] using concatenated protein output from Anvio. AMR genes were predicted with both NCBI AMRFinderPlus (version 4.0.19, with database version 2024-12-18.7 and the *Escherichia*-specific model)[61] and Resistance Gene Identifier (RGI; version 6.0.4 with Comprehensive Antibiotic Resistance Database (CARD), version

3.2.7)[68]. Outputs from AMRFinderPlus and RGI were aggregated together by matching AMR gene names. MLST typing was done with mlst (version 2.19.0)[69,70], Clermont phylogroups were determined using Clermontyping[71], and plasmid mobility type was determined using MOB-suite (version 3.1.9)[72]. For synteny analysis, plasmids were annotated with Bakta Web[73] (software v1.12.0, database v6.0), and annotations were visualized with clinker[74] (v0.0.32).

Genomic database analysis of *E. coli* plasmids

Plasmids from two *E. coli* isolates (SW070910 and SW071620) were analyzed against a database of 40,757 globally distributed plasmids[36], integrated and deduplicated from the following databases: PLSDB (version 2020_11_19)[75], Orlek[76], COMPASS[77], pATLAS[78], and MOB-suite (version 3.0.1)[72]. Plasmids from the Galápagos *E. coli* isolates were compared to this database using command line BLAST+ (version 2.12.0)[79], and all hits with an *E* value ≤ $1e^{-100}$ were considered matches. For plotting BLAST results (Fig. 6D), each plasmid used to query the database was divided into 2000 equally sized regions. For each region, we collected the set of plasmid names (BLAST Subject IDs) from the global database BLAST hits to the region. This set of plasmid names was used as input for visualizing the pairwise Jaccard Similarity Index ($J(A,B) = |A \cap B| / |A \cup B|$) for different regions of the Galápagos plasmids. Identical sets of database plasmid BLAST hits to two regions within a Galápagos plasmid would yield a Jaccard index value of 1, and no common plasmid database plasmid BLAST hits to two regions would yield a Jaccard index value of 0 (Supplementary Fig. 5).

Reporting summary

Further information on research design is available in the Nature Portfolio Reporting Summary linked to this article.

Data availability

Metagenomic sequencing data and whole-genome sequencing data for *E. coli* isolates are available on the Sequence Read Archive (SRA) at accession PRJNA1320681 and PRJNA1320685, respectively. Source data are provided with this paper.

Code availability

All code used for analyses and figure generation is available on GitHub at https://github.com/ruicatxiao/GERA.

References

1. GBD 2021 Antimicrobial Resistance Collaborators Global burden of bacterial antimicrobial resistance 1990-2021: a systematic analysis with forecasts to 2050. *Lancet* **404**, 1199–1226 (2024).
2. Belachew, S. A., Hall, L. & Selvey, L. A. Non-prescription dispensing of antibiotic agents among community drug retail outlets in sub-Saharan African countries: a systematic review and meta-analysis. *Antimicrob. Resist. Infect. Control* **10**, 13 (2021).
3. Lewnard, J. A. et al. Burden of bacterial antimicrobial resistance in low-income and middle-income countries avertible by existing interventions: an evidence review and modelling analysis. *Lancet* **403**, 2439–2454 (2024).
4. Sulis, G., Sayood, S. & Gandra, S. Antimicrobial resistance in low- and middle-income countries: current status and future directions. *Expert Rev. Anti Infect. Ther.* **20**, 147–160 (2022).
5. Okeke, I. N., Lamikanra, A. & Edelman, R. Socioeconomic and behavioral factors leading to acquired bacterial resistance to antibiotics in developing countries. *Emerg. Infect. Dis.* **5**, 18–27 (1999).
6. Faria, N. R. et al. Establishment and cryptic transmission of Zika virus in Brazil and the Americas. *Nature* **546**, 406–410 (2017).
7. Barquero, A., Marini, S., Boucher, C., Ruiz, J. & Prosperi, M. KARGAMobile: Android app for portable, real-time, easily interpretable analysis of antibiotic resistance genes via nanopore sequencing. *Front. Bioeng. Biotechnol.* **10**, 1016408 (2022).
8. Kumari, L. S., Siriwardhana, D. M., Liyanapathirana, V., Jinadasa, R. & Wijesinghe, P. Rapid whole genome sequencing for AMR surveillance in low- and middle-income countries: Oxford Nanopore Technology reveals multidrug-resistant Enterobacter cloacae complex from dairy farms in Sri Lanka. *BMC Vet. Res.* **21**, 351 (2025).
9. Hirabayashi, A. et al. On-site genomic epidemiological analysis of antimicrobial-resistant bacteria in Cambodia with portable laboratory equipment. *Front. Microbiol.* **12**, 675463 (2021).
10. Natale, A. et al. The Mini-Lab: accessible clinical bacteriology for low-resource settings. *Lancet Microbe* **1**, e56–e58 (2020).
11. Caisaguano, F. A. et al. Annual report on visitor arrivals to the protected areas of Galapagos for the year 2022. *Galapagos National Park Directorate*. www.galapagos.gob.ec/wp-content/uploads/2023/05/GNPD-2022-ANNUAL-REPORT.pdf (2023).
12. Burbano, D. V., Valdivieso, J. C., Izurieta, J. C., Meredith, T. C. & Ferri, D. Q. "Rethink and reset" tourism in the Galapagos Islands: stakeholders' views on the sustainability of tourism development. *Ann. Tour. Res. Empir. Insights* **3**, 100057 (2022).
13. Quiroga, D. Crafting nature: the Galapagos and the making and unmaking of a "natural laboratory. *JPE* **16**, 123 (2009).
14. Tuholske, C. et al. Mapping global inputs and impacts from of human sewage in coastal ecosystems. *PLoS ONE* **16**, e0258898 (2021).
15. Lee, J., Ju, F., Beck, K. & Bürgmann, H. Differential effects of wastewater treatment plant effluents on the antibiotic resistomes of diverse river habitats. *ISME J.* **17**, 1993–2002 (2023).
16. Knight, M. E., Farkas, K., Kiss, A. & Jones, D. L. National-scale insights into AMR transmission along the wastewater-environment continuum. *Water Res.* **282**, 123603 (2025).
17. Read, D. S. et al. Dissemination and persistence of antimicrobial resistance (AMR) along the wastewater-river continuum. *Water Res.* **264**, 122204 (2024).
18. Grube, A. M., Stewart, J. R. & Ochoa-Herrera, V. The challenge of achieving safely managed drinking water supply on San Cristobal island, Galápagos. *Int. J. Hyg. Environ. Health* **228**, 113547 (2020).
19. Riascos-Flores, L. et al. Levels and origin of nutrients in the coastal waters of the Galapagos Islands. https://doi.org/10.2139/ssrn.4597361 (2023).
20. Overbey, K. N., Hatcher, S. M. & Stewart, J. R. Water quality and antibiotic resistance at beaches of the Galápagos Islands. *Front. Environ. Sci.* **3**, 64 (2015).
21. Gerhard, W. A., Choi, W. S., Houck, K. M. & Stewart, J. R. Water quality at points-of-use in the Galapagos Islands. *Int. J. Hyg. Environ. Health* **220**, 485–493 (2017).
22. Seurinck, S., Defoirdt, T., Verstraete, W. & Siciliano, S. D. Detection and quantification of the human-specific HF183 Bacteroides 16S rRNA genetic marker with real-time PCR for assessment of human faecal pollution in freshwater. *Environ. Microbiol.* **7**, 249–259 (2005).
23. Newton, R. J. et al. Sewage reflects the microbiomes of human populations. *MBio.* **6**, e02574 (2015).
24. Fouz, N. et al. The contribution of wastewater to the transmission of antimicrobial resistance in the environment: implications of mass gathering settings. *Trop. Med. Infect. Dis.* **5**, 33 (2020).
25. Sambaza, S. S. & Naicker, N. Contribution of wastewater to antimicrobial resistance: a review article. *J. Glob. Antimicrob. Resist.* **34**, 23–29 (2023).
26. Pruden, A., Vikesland, P. J., Davis, B. C. & de Roda Husman, A. M. Seizing the moment: now is the time for integrated global surveillance of antimicrobial resistance in wastewater environments. *Curr. Opin. Microbiol.* **64**, 91–99 (2021).
27. Mahfouz, N., Ferreira, I., Beisken, S., von Haeseler, A. & Posch, A. E. Large-scale assessment of antimicrobial resistance marker databases for genetic phenotype prediction: a systematic review. *J. Antimicrob. Chemother.* **75**, 3099–3108 (2020).

28. Yee, R., Dien Bard, J. & Simner, P. J. The genotype-to-phenotype dilemma: how should laboratories approach discordant susceptibility results? *J. Clin. Microbiol.* **59**, 10–1128 (2021).
29. World Health Organization (WHO). *WHO Bacterial Priority Pathogens List, 2024* (World Health Organization, 2024).
30. Waters, N. R., Abram, F., Brennan, F., Holmes, A. & Pritchard, L. Easy phylotyping of *Escherichia coli* via the EzClermont web app and command-line tool. *Access Microbiol.* **2**, acmi000143 (2020).
31. Larsen, M. V. et al. Multilocus sequence typing of total-genome-sequenced bacteria. *J. Clin. Microbiol.* **50**, 1355–1361 (2012).
32. Fuga, B. et al. WHO critical priority *Escherichia coli* as one health challenge for a post-pandemic scenario: genomic surveillance and analysis of current trends in Brazil. *Microbiol. Spectr.* **10**, e0125621 (2022).
33. Manges, A. R. et al. Global extraintestinal pathogenic *Escherichia coli* (ExPEC) lineages. *Clin. Microbiol. Rev.* **32**, 10–1128 (2019).
34. Manges, A. R. et al. Widespread distribution of urinary tract infections caused by a multidrug-resistant *Escherichia coli* clonal group. *N. Engl. J. Med.* **345**, 1007–1013 (2001).
35. Dimitriu, T., Marchant, L., Buckling, A. & Raymond, B. Bacteria from natural populations transfer plasmids mostly towards their kin. *Proc. Biol. Sci.* **286**, 20191110 (2019).
36. Cazares, A. et al. Pre- and postantibiotic epoch: The historical spread of antimicrobial resistance. *Science* **390**, eadr1522 (2025).
37. Gifford, S. M. et al. Microbial niche diversification in the galápagos archipelago and its response to El Niño. *Front. Microbiol.* **11**, 575194 (2020).
38. Parque Nacional Galápagos. The DPNG initiated administrative sanctioning proceedings for alleged pollution on the beaches of San Cristóbal. https://galapagos.gob.ec/comunicado-oficial-2/ (2024).
39. Djordjevic, S. P. et al. Genomic surveillance for antimicrobial resistance—a One Health perspective. *Nat. Rev. Genet.* **25**, 142–157 (2024).
40. Riofrío-Lazo, M., Arreguín-Sánchez, F. & Páez-Rosas, D. Population abundance of the endangered Galapagos Sea Lion Zalophus wollebaeki in the southeastern Galapagos Archipelago. *PLoS ONE* **12**, e0168829 (2017).
41. Denkinger, J., Quiroga, D. & Murillo, J. C. Assessing human–wildlife conflicts and benefits of Galápagos Sea lions on San Cristóbal Island, Galápagos. In *The Galapagos Marine Reserve* (eds Denkinger, J. & Vinueza, L.) 285–305 (Springer International Publishing, 2014).
42. Thornton, S. M., Nolan, S. & Gulland, F. M. Bacterial isolates from California sea lions (*Zalophus californianus*), harbor seals (*Phoca vitulina*), and northern elephant seals (*Mirounga angustirostris*) admitted to a rehabilitation center along the central California coast, 1994-1995. *J. Zoo. Wildl. Med.* **29**, 171–176 (1998).
43. Kim, J. H. et al. Endocarditis associated with Escherichia coli in a sea lion (*Zalophus californianus*). *J. Vet. Diagn. Invest.* **14**, 260–262 (2002).
44. Delport, T. C., Harcourt, R. G., Beaumont, L. J., Webster, K. N. & Power, M. L. Molecular detection of antibiotic-resistance determinants in *Escherichia coli* isolated from the endangered Australian sea lion (*Neophoca cinerea*). *J. Wildl. Dis.* **51**, 555–563 (2015).
45. Fulham, M., Power, M. & Gray, R. Comparative ecology of *Escherichia coli* in endangered Australian sea lion (*Neophoca cinerea*) pups. *Infect. Genet. Evol.* **62**, 262–269 (2018).
46. Berthe, T., Ratajczak, M., Clermont, O., Denamur, E. & Petit, F. Evidence for coexistence of distinct *Escherichia coli* populations in various aquatic environments and their survival in estuary water. *Appl. Environ. Microbiol.* **79**, 4684–4693 (2013).
47. Erb, I. K. et al. *Escherichia coli* in urban marine sediments: interpreting virulence, biofilm formation, halotolerance, and antibiotic resistance to infer contamination or naturalization. *FEMS Microbes* **5**, xtae024(2024).
48. Baron, S., Hadjadj, L., Rolain, J.-M. & Olaitan, A. O. Molecular mechanisms of polymyxin resistance: knowns and unknowns. *Int. J. Antimicrob. Agents* **48**, 583–591 (2016).
49. Antimicrobial Resistance Collaborators Global burden of bacterial antimicrobial resistance in 2019: a systematic analysis. *Lancet* **399**, 629–655 (2022).
50. Alonso-Del Valle, A. et al. Antimicrobial resistance level and conjugation permissiveness shape plasmid distribution in clinical enterobacteria. *Proc. Natl. Acad. Sci. USA* **120**, e2314135120 (2023).
51. Roth, J. N. & Bontrager, G. L. Temperature-independent pectin gel method for coliform determination in dairy products: collaborative study. *J. AOAC Int.* **72**, 298–302 (1989).
52. O'Connell, K. A. et al. Accelerating genomic workflows using NVIDIA Parabricks. *BMC Bioinforma.* **24**, 221 (2023).
53. Kovaka, S., Fan, Y., Ni, B., Timp, W. & Schatz, M. C. Targeted nanopore sequencing by real-time mapping of raw electrical signal with UNCALLED. *Nat. Biotechnol.* **39**, 431–441 (2021).
54. Loose, M., Malla, S. & Stout, M. Real-time selective sequencing using nanopore technology. *Nat. Methods* **13**, 751–754 (2016).
55. Weilguny, L. et al. Dynamic, adaptive sampling during nanopore sequencing using Bayesian experimental design. *Nat. Biotechnol.* **41**, 1018–1025 (2023).
56. Faria, N. R. et al. Mobile real-time surveillance of Zika virus in Brazil. *Genome Med.* **8**, 97 (2016).
57. Tegally, H. et al. The evolving SARS-CoV-2 epidemic in Africa: insights from rapidly expanding genomic surveillance. *Science* **378**, eabq5358 (2022).
58. Simmonds, S. E. et al. CZ ID: a cloud-based, no-code platform enabling advanced long read metagenomic analysis. Preprint at *bioRxiv* https://doi.org/10.1101/2024.02.29.579666 (2024).
59. Kolmogorov, M. et al. metaFlye: scalable long-read metagenome assembly using repeat graphs. *Nat. Methods* **17**, 1103–1110 (2020).
60. Hackl, T. et al. proovframe: frameshift-correction for long-read (meta)genomics. Preprint at https://www.biorxiv.org/content/10.1101/2021.08.23.457338v1 (2021).
61. Feldgarden, M. et al. AMRFinderPlus and the Reference Gene Catalog facilitate examination of the genomic links among antimicrobial resistance, stress response, and virulence. *Sci. Rep.* **11**, 12728 (2021).
62. CLSI. *CLSI. Performance Standards for Antimicrobial Susceptibility Testing* (CLSI, 2025).
63. Wick, R. R., Howden, B. P. & Stinear, T. P. Autocycler: long-read consensus assembly for bacterial genomes. *Bioinformatics* **41**, btaf474 (2025).
64. Li, H. Minimap and miniasm: fast mapping and de novo assembly for noisy long sequences. *Bioinformatics* **32**, 2103–2110 (2016).
65. Vaser, R. & Šikić, M. Time- and memory-efficient genome assembly with Raven. *Nat. Comput. Sci.* https://doi.org/10.1038/s43588-021-00073-4 (2021).
66. Eren, A. M. et al. Community-led, integrated, reproducible multi-omics with anvi'o. *Nat. Microbiol.* **6**, 3–6 (2021).
67. Ronquist, F. et al. MrBayes 3.2: efficient Bayesian phylogenetic inference and model choice across a large model space. *Syst. Biol.* **61**, 539–542 (2012).
68. Alcock, B. P. et al. CARD 2023: expanded curation, support for machine learning, and resistome prediction at the Comprehensive Antibiotic Resistance Database. *Nucleic Acids Res.* **51**, D690–D699 (2023).
69. Jolley, K. A., Bray, J. E. & Maiden, M. C. J. Open-access bacterial population genomics: BIGSdb software, the PubMLST.org website and their applications. *Wellcome Open Res.* **3**, 124 (2018).
70. Jolley, K. A. & Maiden, M. C. J. BIGSdb: scalable analysis of bacterial genome variation at the population level. *BMC Bioinforma.* **11**, 595 (2010).

71. Beghain, J., Bridier-Nahmias, A., Le Nagard, H., Denamur, E. & Clermont, O. ClermonTyping: an easy-to-use and accurate in silico method for *Escherichia* genus strain phylotyping. *Microb. Genom.* **4**, e000192 (2018).
72. Robertson, J. & Nash, J. H. E. MOB-suite: software tools for clustering, reconstruction and typing of plasmids from draft assemblies. *Microb. Genom.* **4**, e000206(2018).
73. Beyvers, S., Jelonek, L., Goesmann, A. & Schwengers, O. Bakta Web—rapid and standardized genome annotation on scalable infrastructures. *Nucleic Acids Res.* **53**, W51–W56 (2025).
74. Gilchrist, C. L. M. & Chooi, Y.-H. clinker & clustermap.js: automatic generation of gene cluster comparison figures. *Bioinformatics* **37**, 2473–2475 (2021).
75. Galata, V., Fehlmann, T., Backes, C. & Keller, A. PLSDB: a resource of complete bacterial plasmids. *Nucleic Acids Res.* **47**, D195–D202 (2019).
76. Orlek, A. et al. A curated dataset of complete Enterobacteriaceae plasmids compiled from the NCBI nucleotide database. *Data Brief.* **12**, 423–426 (2017).
77. Douarre, P.-E., Mallet, L., Radomski, N., Felten, A. & Mistou, M.-Y. Analysis of COMPASS, a new comprehensive plasmid database revealed prevalence of multireplicon and extensive diversity of IncF plasmids. *Front. Microbiol.* **11**, 483 (2020).
78. Jesus, T. F. et al. Plasmid ATLAS: plasmid visual analytics and identification in high-throughput sequencing data. *Nucleic Acids Res.* **47**, D188–D194 (2019).
79. Camacho, C. et al. BLAST + : architecture and applications. *BMC Bioinforma.* **10**, 421 (2009).

Acknowledgements

We thank Fausto Rodriguez for facilitating access to the Galápagos National Park; Whitman Cox for providing guidance on wastewater management infrastructure and challenges on San Cristóbal island; and Demy Castillo for testing qPCR protocols on the island and providing feedback on assay usability. We also thank Jesse vanWestrienen and Max Pearlman from Biomeme, Inc., for guidance on qPCR assay selection and water collection and filtration strategies.

Author contributions

D.P.B. and L.M.M. designed and oversaw all experiments. A.L., J.C.R., K.V., M.M., M.T., L.E., N.P.J. and K.G. carried out all field work and experiments and participated in data analysis. A.L. and L.M.M. generated and analyzed sequencing data. R.X. analyzed sequencing data and assisted with figure preparation. D.P.B. and L.L.M. trained undergraduate students. L.M.M., L.E., M.T., and K.P.K. supervised undergraduate researchers during field work and assisted with all field work. S.D.C. assisted with the development, optimization, and interpretation of Kirby–Bauer disk assays. M.W. and E.V. managed programmatic aspects of the work and coordinated undergraduate recruitment, instruction, and mentoring. W.C. provided space and resources for a temporary laboratory set-up. E.V. facilitated access to National Park sites and provided guidance on water collection sites and wastewater management on the island. D.P.B., L.M.M., and A.L. wrote the manuscript. All authors reviewed the manuscript, provided feedback and revisions, and approved the final version for publication. All authors have given their consent for publication.

Funding

M.W. and E.V. disclose support for the research of this work from the National Science Foundation (grant number STS-1557138). M.W., M.T., and K.P.K. disclose support for the research of this work from the School of Arts and Sciences and the Penn Global Research Institute at the University of Pennsylvania. M.M., N.P.J., and K.G. disclose support for the research of this work from the University of Pennsylvania's Center for Undergraduate Research Foundation (CURF) Grants for Faculty Mentoring Undergraduate Research (GfFMUR) in 2023 and 2024. A.L. discloses support for the research of this work from the University of Pennsylvania's Roy and Diana Vagelos Science Challenge Award in 2022–2023 and the Samvid Scholarship in 2024–2026. L.M.M. and D.P.B. disclose support for the research of this work from the University of Pennsylvania's Institute for Infectious and Zoonotic Diseases (IIZD) pilot grant program.

Competing interests

The authors declare no competing interests.

Additional information

Supplementary information The online version contains supplementary material available at https://doi.org/10.1038/s41467-026-74899-9.

Correspondence and requests for materials should be addressed to Lisa M. Mattei or Daniel P. Beiting.

Peer review information *Nature Communications* thanks Amy Pruden and the other anonymous reviewer(s) for their contribution to the peer review of this work. A peer review file is available.

[1]Department of Pathobiology, School of Veterinary Medicine, University of Pennsylvania, Philadelphia, PA, USA. [2]Harvard Medical School, Boston, MA, USA. [3]Galápagos Education and Research Alliance, Penn Global Research Institute, University of Pennsylvania, Philadelphia, PA, USA. [4]Department of Philosophy, School of Arts and Sciences, University of Pennsylvania, Philadelphia, PA, USA. [5]Parque Nacional Galápagos, Isla San Cristóbal, Galápagos, Ecuador. [6]Perry World House, University of Pennsylvania, Philadelphia, PA, USA. [7]These authors jointly supervised this work: Lisa M. Mattei, Daniel P. Beiting.
✉e-mail: lmattei@upenn.edu; beiting@upenn.edu